Lecture 27 Second Order Nonlinear Optics

Anharmonic potential with no inversion symmetry

Previously we have considered so-called harmonic potentials, described by symmetric potential $U(x) = -U_0 + Kx^2/2$. This potential, shown in Fig.27.1a obviously has a center of inversion symmetry, i.e. $U(x) = U(-x)$. But what if the crystalline lattice is such that it does not have a center of inversion symmetry, such as one shown in Fig.27.1b where electron sees different environments on the left and on the right. Then $U(x) \neq U(-x)$ and the potential expansion into power series will have odd order terms, the lowest of which is the third order one as shown in Fig.27.1a

$$U(x) = -U_0 + \frac{Kx^2}{2} + \frac{Lx^3}{3} + ... \tag{27.1}$$

The equation of motion then can be written as

$$m_0 \frac{d^2x}{dt^2} = -Kx - Lx^2 + ... \tag{27.2}$$

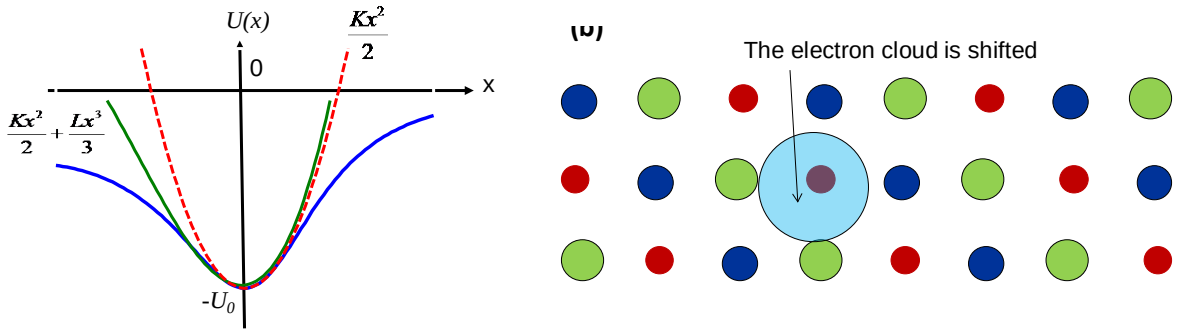

Figure 27.1 (a) Harmonic (red) and anharmonic (blue) potentials (b) Crystalline lattice without inversion symmetry.

Consider now this anharmonic oscillator being excited by a two-tone field, i.e. field with two frequencies $\omega_{1,2}$

$$E(t) = E_1 e^{-j\omega_1 t} + E_2 e^{-j\omega_2 t} + c.c. \tag{27.3}$$

And substitute it into the equation of motion

$$m_0 \frac{d^2x}{dt^2} = -m_0\omega_0^2 x - Lx^2 - eE(t) \tag{27.4}$$

where $\omega_0 = \sqrt{K/m_0}$ is the resonant frequency. We shall look for the solution now that combines both first and second order terms

$$\begin{aligned} x(t) &= a_1 E_1 e^{-j\omega_1 t} + a_2 E_2 e^{-j\omega_2 t} + c.c. \\ &+ b_1 E_1^2 e^{-2j\omega_1 t} + b_2 E_1^2 e^{-2j\omega_2 t} + c.c. \\ &+ c_+ E_1 E_2 e^{-j(\omega_1+\omega_2)t} + c_- E_1 E_2^* e^{-j(\omega_1-\omega_2)t} + c.c. \\ &+ c_1 E_1^* E_1 + c_2 E_2^* E_2 \end{aligned} \tag{27.5}$$

The frist line has linear response, the second line is second harmonic generation (SHG), the third line contains sun and difference frequency generation terms (SFG and DFG), and, finally the last line corresponds to optical rectification, i.e. generation of DC poalrization. We can now find the square of (27.5), keeing only the second order terms, i..e the terms containing $a_i a_j$ but not the higher order terms

$$\begin{aligned} x^2(t) &= (a_1 E_1 e^{-j\omega_1 t} + a_2 E_2 e^{-j\omega_2 t} + c.c.)^2 = \\ &= a_1^2 E_1^2 e^{-2j\omega_1 t} + a_2^2 E_2^2 e^{-2j\omega_2 t} + c.c. \\ &+ 2a_1 a_2 E_1 E_2 e^{-j(\omega_1+\omega_2)t} + 2a_1 a_2^* E_1 E_2^* e^{-j(\omega_1-\omega_2)t} + c.c. \\ &+ 2a_1 a_1^* E_1^* E_1 + 2a_2 a_2^* E_2^* E_2 \end{aligned} \tag{27.6}$$

Now, re-write (27.4) as

$$\omega_0^2 x + \frac{d^2 x}{dt^2} = -\frac{L}{m_0} x^2 - \frac{e}{m_0} E(t), \tag{27.7}$$

substitute (27.5) and (27.6) into it and combine the terms with the same temporal dependencies. First we combine the terms with $\exp(-j\omega_{1,2}t)$

$$a_{1,2}(\omega_0^2 - \omega_{1,2}^2) E_{1,2} e^{-j\omega_{1,2}t} = -\frac{e}{m_0} E_{1,2} e^{-j\omega_{1,2}t} \tag{27.8}$$

And obtain the expected linear response

$$a_{1,2} = -\frac{e}{m_0(\omega_0^2 - \omega_{1,2}^2)} \tag{27.9}$$

Then we combine second harmonic terms $\exp(-j2\omega_{1,2}t)$

$$b_{1,2}(\omega_0^2 - 4\omega_{1,2}^2) E_{1,2}^2 e^{-2j\omega_{1,2}t} = -\frac{L}{m_0} a_{1,2}^2 E_{1,2}^2 e^{-2j\omega_{1,2}t} \tag{27.10}$$

and obtain SH response

$$b_{1,2} = -\frac{L}{m_0} \frac{a_{1,2}^2}{\omega_0^2 - 4\omega_{1,2}^2} = \frac{e^2 L}{m_0^3 (\omega_0^2 - \omega_{1,2}^2)^2 \left(\omega_0^2 - 4\omega_{1,2}^2\right)} \tag{27.11}$$

Then we move on to SFG and DFG

$$c_+\left[\omega_0^2-(\omega_1+\omega_2)^2\right]E_1E_2e^{-j(\omega_1+\omega_2)t}=-\frac{2L}{m_0}a_{1,2}^2E_1E_2e^{-j(\omega_1+\omega_2)t}$$
$$c_-\left[\omega_0^2-(\omega_1-\omega_2)^2\right]E_1E_2^*e^{-j(\omega_1-\omega_2)t}=-\frac{2L}{m_0}a_{1,2}^2E_1E_2^*e^{-j(\omega_1-\omega_2)t} \quad (27.12)$$

So that

$$c_\pm=\frac{2e^2L}{m_0^3(\omega_0^2-\omega_1^2)(\omega_0^2-\omega_2^2)\left[\omega_0^2-(\omega_1\pm\omega_2)^2\right]} \quad (27.13)$$

Finally, for DC terms we obtain

$$c_{1,2}\omega_0^2E_{1,2}^*E_{1,2}=-\frac{2L}{m_0}a_{1,2}^2E_{1,2}^*E_{1,2} \quad (27.14)$$

and

$$c_{1,2}=\frac{2e^2L}{m_0^3(\omega_0^2-\omega_{1,2}^2)^2\omega_0^2} \quad (27.15)$$

Second order susceptibility

Consider now the polarization of the medium that will have terms proportional to all the coefficients above. For instance, for SHG we shall have (27.10)

$$P(2\omega_{1(2)})=-Neb_{1(2)}e^{-j2\omega_{1(2)}t}=\varepsilon_0\chi^{(2)}(2\omega_{1(2)};\omega_{1(2)},\omega_{1(2)})E_{1(2)}^2e^{-j2\omega_{1(2)}t}+c.c. \quad (27.16)$$

where we introduced second order polarizability fro SHG

$$\chi^{(2)}(2\omega;\omega,\omega)\equiv d(\omega)=\frac{Ne^3L}{\varepsilon_0m_0^3(\omega_0^2-\omega^2)^2\left(\omega_0^2-4\omega^2\right)} \quad (27.17)$$

$d(\omega)$ being an SHG coefficient.

For SFG and DFG we obtain from (27.12)

$$P(\omega_1\pm\omega_2)=-Nec_\pm e^{-j(\omega_1\pm\omega_2)t}=2\varepsilon_0\chi^{(2)}(\omega_1\pm\omega_2;\omega_1,\omega_2)E_1E_2^{(*)}e^{-j(\omega_1\pm\omega_2)t}+c.c. \quad (27.18)$$

A factor oftwo 2 is here because one can change indices 1 and 2. The nonlinear susceptibilities for SFH and DFG are

$$\chi^{(2)}(\omega_1\pm\omega_2;\omega_1,\omega_2)=\frac{Ne^3L}{\varepsilon_0m_0^3(\omega_0^2-\omega_1^2)(\omega_0^2-\omega_2^2)\left[\omega_0^2-(\omega_1\pm\omega_2)^2\right]} \quad (27.19)$$

Finally, for optical rectification

$$P(0) = -Nec_1 = 2\varepsilon_0 \chi^{(2)}(0;\omega_1,\omega_1)E_1 E_2^{(*)} + c.c. \tag{27.20}$$

A factor of two is because you have $EE^* + E^*E$. The susceptibility is

$$\chi^{(2)}(0;\omega,\omega) = \frac{Ne^3 L}{\varepsilon_0 m_0^3(\omega_0^2 - \omega^2)^2 \omega_0^2} \tag{27.21}$$

If one goes back to Lecture 24 on Electro-Optic effect (Eq 24.20) we can see that optical rectification has the same susceptibility as linear electro-optic effect. In fact, OR is the reverse effect to linear reflector-optic effect and

$$\chi^{(2)}(0;\omega,\omega) = \chi^{(2)}(\omega;0,\omega)\frac{Ne^3 L}{\varepsilon_0 m_0^3(\omega_0^2 - \omega^2)^2 \omega_0^2} \tag{27.22}$$

One should note that both OR and EO effect also include motion of ions so those susceptibilities can be quite different from the SFG and DFG when all three frequencies are in optical range. SHG is of course a special case of SFG for $\omega_1 = \omega_2$. Although SFG and SHG coefficients have different frequency dependences, for the nearly degenerate SFG when frequencies are close $\omega_1 \approx \omega_2$ one has $\chi^{(2)}(\omega_1 + \omega_2;\omega_1,\omega_2) \approx d(\omega_1)$. Similarly, for nearly degenerate DFG when $\omega_1 \approx 2\omega_2$ one can approximate $\chi^{(2)}(\omega_1 - \omega_2;\omega_1,\omega_2) \approx d(\omega_2)$.

All prior derivations where done for the one dimensional case in which polarization is always parallel to the field and one can use scale notation. But, more generally we are dealing with vectors and therefore d is a third-rank tensor and

$$\mathbf{P}^{(2)} = \varepsilon_0 d\mathbf{EE}, \tag{27.23}$$

or

$$P_k^{(2)} = \varepsilon_0 \sum_{i,j=x,y,z} d_{ijk} E_i E_j \tag{27.24}$$

If we re-write the outer product of the vectors as a 1x6 vector,

$$\mathbf{EE} \equiv \mathbf{E} \otimes \mathbf{E} = \begin{pmatrix} E_x^2 & E_x E_y & E_x E_z \\ E_x E_y & E_y^2 & E_y E_z \\ E_x E_z & E_y E_z & E_z^2 \end{pmatrix} \Rightarrow \begin{pmatrix} E_x^2 \\ E_y^2 \\ E_z^2 \\ 2E_{yz} \\ 2E_{xz} \\ 2E_{xy} \end{pmatrix} \tag{27.25}$$

The third-rank tensor of d can be written as 3x6 second rank tensor, and nonlinear polarization becomes

$$\mathbf{P}^{(2)} = \begin{pmatrix} P_x^{(2)} \\ P_y^{(2)} \\ P_z^{(2)} \end{pmatrix} = \varepsilon_0 \begin{pmatrix} d_{11} & d_{12} & d_{13} & d_{14} & d_{15} & d_{16} \\ d_{21} & d_{22} & d_{23} & d_{24} & d_{25} & d_{26} \\ d_{31} & d_{32} & d_{33} & d_{34} & d_{35} & d_{36} \end{pmatrix} \begin{pmatrix} E_x^2 \\ E_y^2 \\ E_y^2 \\ 2E_{yz} \\ 2E_{xz} \\ 2E_{xy} \end{pmatrix} \tag{27.26}$$

Consider the SHG coefficients of the more important crystals used in nonlinear optics. Historically the crystals of Potassium dihydrogen phosphate KH_2PO_4 , known as KDP and potassium dideuterium phosphate KD_2PO_4 known as KD*P were the first one to be used. The tensor of nonlinear susceptibility has only three non-zero coefficients with values $d_{36} \sim d_{14} \approx 0.36\, pm/V$ at $\lambda = 500nm$.

$$d = \begin{pmatrix} 0 & 0 & 0 & d_{14} & 0 & 0 \\ 0 & 0 & 0 & 0 & d_{14} & 0 \\ 0 & 0 & 0 & 0 & 0 & d_{36} \end{pmatrix} \tag{27.27}$$

In mid IR one uses silver gallium selenide $AgGaSe_2$ with the same crystalline structure and much larger coefficients, $d_{36} \sim d_{14} \approx 50\, pm/V$ at $\lambda = 10\mu m$. Note that for materials that are transparent through the entire IR-Visible region nonlinear susceptibity is smaller than for the material which absorb visible light. More on that later.

The most widely used in visible and near IR nonlinear material; is lithium niobate $LiNbO_3$ with a perovskite crystal structure. It has quite a few non-zero coefficients

$$d = \begin{pmatrix} 0 & 0 & 0 & 0 & d_{15} & -d_{22} \\ -d_{22} & d_{22} & 0 & d_{15} & 0 & 0 \\ d_{31} & d_{31} & d_{33} & 0 & 0 & 0 \end{pmatrix} \tag{27.28}$$

with some of them fairly large, $d_{31} \approx -5\, pm/V, d_{33} \approx -30\, pm/V, d_{22} \approx -4\, pm/V$ at $\lambda = 1\mu m$. In the UV one uses beta-Barium borate BaB_2O_4 (BBO) with the same perovskite structure and largest nonlinear coefficient $d_{22} = 4\, pm/V$ at $\lambda = 0.5\mu m$.

Another popular nonlinear material in the visible is Potassium Titanyl Phosphate $KTiPO_4$ or KTP also with quite a few non-zero coefficients,

$$d = \begin{pmatrix} 0 & 0 & 0 & 0 & d_{15} & 0 \\ 0 & 0 & 0 & d_{24} & 0 & 0 \\ d_{31} & d_{31} & d_{33} & 0 & 0 & 0 \end{pmatrix} \tag{27.29}$$

The coefficients are $d_{15} = 1.9\ pm/V$, $d_{24} = 4.2\ pm/V$, $d_{31} = 2.2\ pm/V$, $d_{32} = 2.7\ pm/V$, and the largest one $d_{33} = 17.4\ pm/V$ at $\lambda = 0.7\mu m$.

Other interesting nonlinear optical material are zinc blende III-V and II-VO, such as, for instance GaAs with three equal non-zero coefficients

$$d = \begin{pmatrix} 0 & 0 & 0 & d_{14} & 0 & 0 \\ 0 & 0 & 0 & 0 & d_{14} & 0 \\ 0 & 0 & 0 & 0 & 0 & d_{14} \end{pmatrix} \tag{27.30}$$

For GaAs coefficient d_{14} =140 pm/V at λ=2.0μm is very large but this material is not used because it is very difficult to phase match (see below) .

It is important to note that different materials have different transparency ranges as shown in Fig.27.2.a. It is interesting to see how the transparency range and values of $\chi^{(2)}$ are elated.

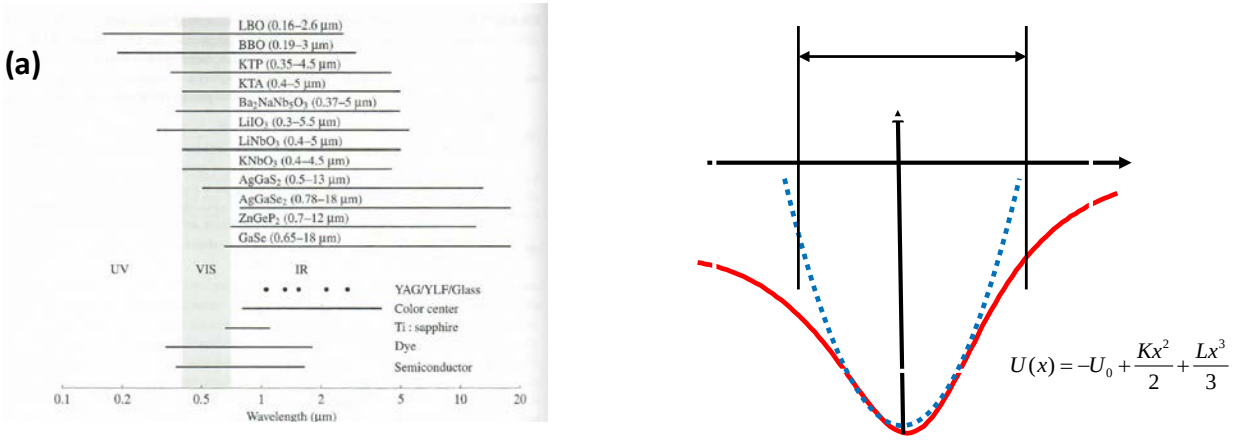

Figure 27.2. (a) Transparency ranges for different second order nonlinear optical materials (b) Model explaining order of magnitude of $\chi^{(2)}$ and its frequency dependence

Order of magnitude of $\chi^{(2)}$ and its dependence on transmission range

Consider once again anharmonic potential, re-drawn in Fig.27.2.b where the size of electronic cloud (i.e. the range in which the electron can move) is a_0. When $x \sim a_0$ the atom (molecule) gets ionized as the bond keeping electron in its place gets broken. Therefore $U(a_0) \approx -U_0 + Ka_0^2/2 \approx 0$. Thus

$$K = m\omega_0^2 \approx U_0 / a_0^2 \tag{27.31}$$

Also, the nonlinear terms become comparable to linear terms when the electron is about to ionize $La_0^3/3 \approx Ka_0^2/2$, and

$$L < U_0 / a_0^3 \tag{27.32}$$

As long as one operates well below the resonance, $\omega << \omega_0$ we have $\omega_0 - \omega \approx \omega_0$ and the expression for off-resonant second order susceptibility is

$$\chi^{(2)}_{nres} \approx \frac{Ne^3 L}{\varepsilon_0 m_0^3 \omega_0^6} < \frac{Ne^2}{\varepsilon_0 m_0 \omega_0^2} \frac{eU_0}{m_0^2 \omega_0^4 a_0^3} \tag{27.33}$$

The first term in (27.33) is (off-resonant) linear susceptibility $\chi^{(1)} = n^2 - 1$, In the second term we substitute (27.31) and obtain as a result

$$\chi^{(2)}_{nres} < (n^2 - 1) \frac{eU_0}{U_0^2 / a_0} = (n^2 - 1) \frac{ea_0}{U_0} = (n^2 - 1) F_a^{-1} \tag{27.34}$$

where

$$F_a = U_0 / ea_0 \sim 10^{10} - 10^{11} V / m \tag{27.35}$$

Is the "intrinsic" or "atomic" field that binds the electron. Therefore, maximum value of $\chi^{(2)}$ is $10^{-10} - 10^{-9} m / V$ depending on and U_0 In order to find the frequency dependence we substitute (27.31) into the entire denominator in (27.33) and obtain

$$\chi^{(2)}_{nres} < \frac{Ne^3 a_0^3}{\varepsilon_0 U_0^2} \sim A \frac{e^3}{\varepsilon_0 U_0^2} \tag{27.36}$$

Where $A = Na_0^3$ is the packing density (filling fraction) that is on the order of unity. From quantum mechanics it follows that the deeper is the potential well the larger is resonant frequency ω_0, although we cannot really establish the exact dependence. So, overall as ω_0 increases and thus the transparency region expands the nonlinear susceptibility decreases dramatically. One may say that with optimum asymmetry the maximum value of $\chi^{(2)}$ in the spectral region defined by shortest (transparency) wavelength $\lambda_{tran} \sim 1 / U_0$ increases as roughly λ^2_{tran} .That is why in UV region it is only a few pm/V and in IR can be easily 100's of pm/V.

Second Harmonic generation

Consider now how the SH is generated as shown in Fig.27.3a. Two waves, fundamental

$$\mathbf{E}_1(z,t) = A_1(z) \hat{\mathbf{e}}_1 e^{j(k_1 z - \omega t)} + c.c.;\ k_1 = \omega n_1 / c \tag{27.37}$$

and SH

$$\mathbf{E}_2(z,t) = A_2(z) \hat{\mathbf{e}}_2 e^{j(k_2 z - 2\omega t)} + c.c.;\ k_2 = 2\omega n_2 / c \tag{27.38}$$

where $A_i(z)$ is the amplitude and $\hat{\mathbf{e}}_i$ is the unit vector defining polarization, propagate along the direction z as shown in Fig.27.3.a. The amplitudes are assumed to be slow variables, that do not change much on the scale of a few wavelengths, i.e. formally

$$\frac{\partial^2 A_i}{\partial z^2} << k_i \frac{\partial A_i}{\partial z} \tag{27.39}$$

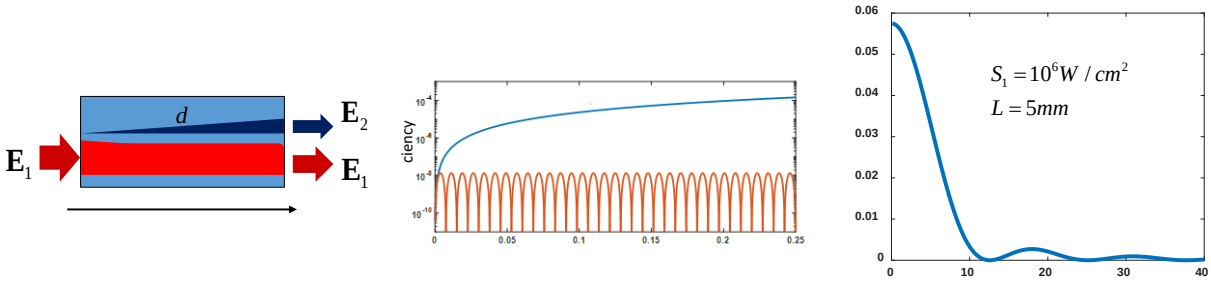

Figure 27.3 (a) Geometry of SHG generation (b) SHG efficiency with and without phase mismatch (c) Efficiency dependence on wavevector mismatch.

The nonlinear polarization at frequency 2ω according to (27.23) is

$$\mathbf{P}_2^{(2)} = \varepsilon_0 d\mathbf{E}_1\mathbf{E}_1 = \varepsilon_0 \left[d\hat{\mathbf{e}}_1\hat{\mathbf{e}}_1\right] A_1^2(z)e^{j(2kz-2\omega t)} \tag{27.40}$$

and the displacement at frequency 2ω is

$$\mathbf{D}_2 = \varepsilon_0 n_2^2 \mathbf{E}_2 + \mathbf{P}_2^{(2)} \tag{27.41}$$

Substituting (27.41) into the wave equation for SH wave

$$\frac{d^2}{dz^2}\mathbf{E}_2 - \frac{1}{\varepsilon_0 c^2}\frac{d^2}{dt^2}\mathbf{D}_2 = 0 \tag{27.42}$$

we obtain,

$$\frac{d^2}{dz^2}\mathbf{E}_2 - \frac{n_2^2}{c^2}\frac{d^2}{dt^2}\mathbf{E}_2 = \frac{1}{\varepsilon_0 c^2}\frac{d^2}{dt^2}\mathbf{P}_2^{(2)} \tag{27.43}$$

On the left hand side, we have the "free wave" propagation and on right hand side we have a nonlinear source. Dot multiply (27.43) by unit vector $\hat{\mathbf{e}}_2$ and obtain

$$\frac{d^2}{dz^2}E_2 - \frac{n_2^2}{c^2}\frac{d^2}{dt^2}E_2 = \frac{1}{\varepsilon_0 c^2}\frac{d^2}{dt^2}\mathbf{P}_2^{(2)} \cdot \hat{\mathbf{e}}_2 \tag{27.44}$$

Use (27.40) and introduce the (scalar) effective SH coefficient

$$d_{eff} = \hat{\mathbf{e}}_2 \cdot \left[d\hat{\mathbf{e}}_1 \otimes \hat{\mathbf{e}}_1\right] \tag{27.45}$$

To obtain

$$\mathbf{P}_2^{(2)} \cdot \hat{\mathbf{e}}_2 = \varepsilon_0 \hat{\mathbf{e}}_2 \cdot \left[d\hat{\mathbf{e}}_1 \otimes \hat{\mathbf{e}}_1\right] A_1^2(z)e^{j(2k_1 z-2\omega t)} = \varepsilon_0 d_{eff} A_1^2(z)e^{j(2k_1 z-2\omega t)} \tag{27.46}$$

Substituting this expression into (27.44) , using (27.39) to neglect second derivative as well as definition of $k_2 = 2n_2\omega / c$ we arrive at

$$\left[\frac{d^2 A_2}{dz^2} + 2jk_2 \frac{dA_2}{dz} - k_2^2 A_2 + \frac{n_2^2}{c^2}(2\omega)^2 A_2 \right] e^{j(k_2 z - 2\omega t)} = -\frac{(2\omega)^2}{c^2} d_{eff} A_1^2(z) e^{j(2k_1 z - 2\omega t)} \qquad (27.47)$$

or

$$\frac{dA_2}{dz} = j\frac{(2\omega)^2}{2k_2 c^2} d_{eff} A_1^2(z) e^{j\Delta kz} = j\kappa A_1^2(z) e^{j\Delta kz} \qquad (27.48)$$

Where we have introduced effective coupling coefficient

$$\kappa = \frac{(2\omega)^2}{2k_2 c^2} d_{eff} = \frac{2\omega}{n_2 c} d_{eff} \qquad (27.49)$$

And the wave-vector (momentum) mismatch

$$\Delta k = 2k_1 - k_2 = 2\frac{\omega}{c}(n_1 - n_2) \qquad (27.50)$$

To start with we assume that the fundamental (or pump) wave does not get depleted and its amplitude A_1 stays constant. Then (27.48) can be easily integrated from one end to another

$$A_2(L) = j\kappa A_1^2 \int_0^L e^{j\Delta kz} dz = j\kappa A_1^2 \frac{e^{j\Delta kL} - 1}{j\Delta k} = je^{j\Delta kL} \frac{\sin(\Delta kL/2)}{\Delta kL/2} \kappa L A_1^2 \qquad (27.51)$$

or

$$\left|A_2(L)\right|^2 = \frac{\sin^2(\Delta kL/2)}{(\Delta kL/2)^2} \kappa^2 L^2 \left(\left|A_1\right|^2 \right)^2 \qquad (27.52)$$

The power densities of the fundamental and SH waves (27.37) and (27.38) are

$$S_{1,2} = \frac{2n_{1,2}}{\eta_0} \left|A_{1,2}\right|^2 \qquad (27.53)$$

(factor of two instead of ½ is because the way we write (27.37) and (27.38) these waves are $E_{1,2} = 2A_{1,2}\cos(k_{1,2}z - \omega_{1,2}t)$). Substituting (27.49) and (27.53) into (27.52) we obtain

$$\frac{S_2(L)\eta_0}{2n_2} = \left(\frac{2\omega}{n_2 c} d_{eff} L \right)^2 \left(\frac{S_1 \eta_0}{2n_1} \right)^2 \frac{\sin^2(\Delta kL/2)}{(\Delta kL/2)^2} \qquad (27.54)$$

and

$$S_2(L) = \frac{2\omega^2 d_{eff}^2 \eta_0}{n_2 n_1^2 c^2} L^2 S_1^2 \frac{\sin^2(\Delta kL/2)}{(\Delta kL/2)^2} = \eta'_{SHG} L^2 S_1^2 \frac{\sin^2(\Delta kL/2)}{(\Delta kL/2)^2} \quad (27.55)$$

Where we have introduced relative SHG efficiency in units of W^{-1} as

$$\eta'_{SHG} = \frac{2\pi^2 d_{eff}^2 \eta_0}{\lambda_2^2 n_2 n_1^2} \quad (27.56)$$

The SHG efficiency itself is

$$\frac{S_2(L)}{S_1} = \eta'_{SHG} L^2 S_1 \frac{\sin^2(\Delta kL/2)}{(\Delta kL/2)^2} \quad (27.57)$$

The SHG efficiency is plotted versus the interaction length L in Fig.27.3.b for $LiNbO_3$ with the following parameters

$$\begin{aligned} &\lambda_1 = 1060nm \ \lambda_2 = 530nm \\ &d_{33} = 30\,pm/V \\ &n_1 = n_e(\lambda_1) = 2.15 \\ &n_2 = n_e(\lambda_2) = 2.22 \end{aligned} \quad (27.58)$$

So that relative SHG efficiency is $\eta'_{SHG} \approx 2.3\times10^{-6} W^{-1}$ and wavevector mismatch $\Delta k = 8300 cm^{-1}$. The pump power density $S_1 = 10^6 W/cm^2$. As one can see the efficiency, i…e SH power oscillates with a half period $L_{coh} = \pi/\Delta k \approx 3.8\mu m$, called the coherence length , which is defined as a length over which the "free propagating wave" E_2 and the "induced" or polarization wave $P_2^{(2)}$ get 180 degrees out of phase. As one can see also in the same figure, if the wavevectors were perfectly matched, the SHG efficiency would continue to increase. The same can be concluded from Fig.27.3.c showing the SHG efficiency for a fixed length of 5mm and different wavevector mismatches.

So the wave vector (phase) matching is necessary and is indeed achieved in, for example green laser pointer shown in Fig.27.4. In this device a semiconductor diode laser pumps Nd:YVO_4 laser crystal emitting at 1064nm and KTP crystal doubles it to 532nm with high efficiency of cR to Visible conversion (up to 30%)

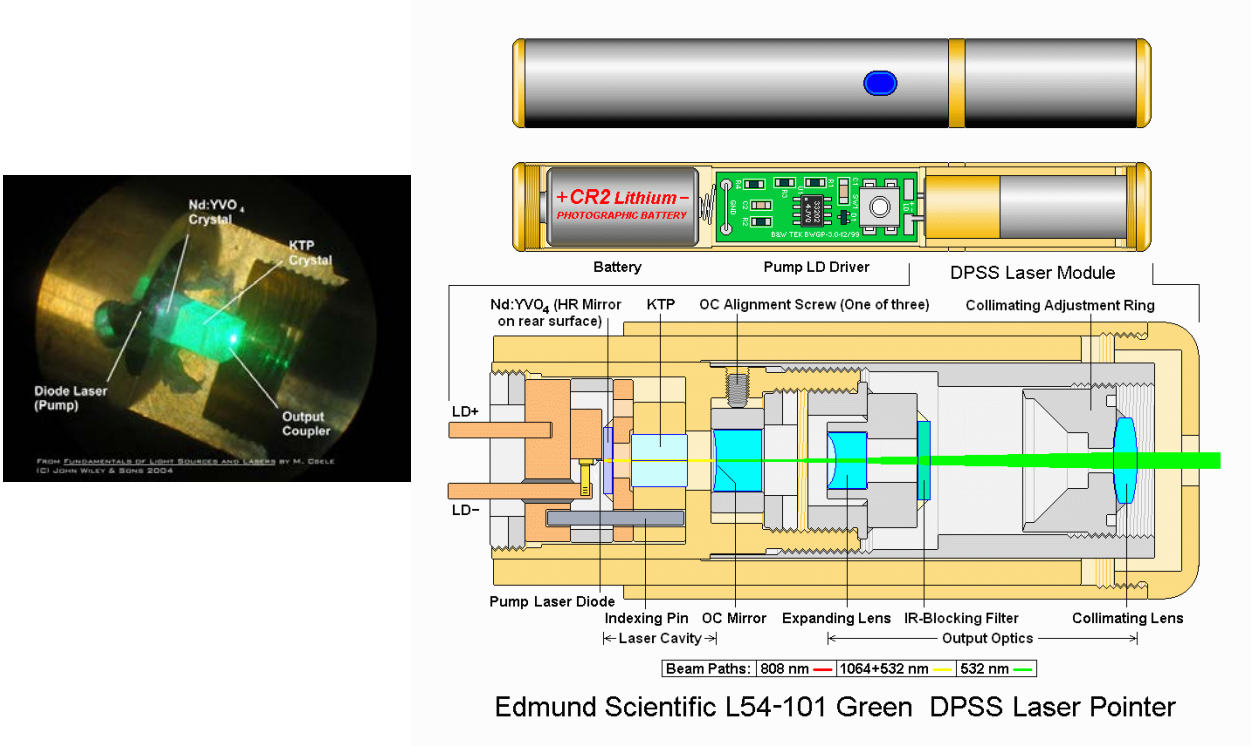

Figure 27.4 Green laser pointer

Phase matching in birefringent crystals

The phase matching condition is

$$\Delta k = 2k_1 - k_2 = 2\frac{\omega}{c}(n_1 - n_2) = 0 \tag{27.59}$$

But in any material with normal dispersion one has $n_2 \equiv n(2\omega) > n(\omega) \equiv n_1$. That is true as long as one considers only isotropic materials, but in anisotropic material's considered in Chapter 22 the light with different polarizations propagate with different phase velocities. Consider for example KDP and let us see how one can double the red light of the Ruby laser with $\lambda_1 = 694.3nm$ into UV light $\lambda_2 = 347.2nm$. The refractive indices for ordinary and extraordinary polarizations are

$$\begin{aligned} n_{1,o} &= 1.50502 \; n_{1,e} = 1.46532 \\ n_{2,o} &= 1.53269 \; n_{2,e} = 1.48711 \end{aligned} \tag{27.60}$$

Since $n_{1,o} > n_{2,e}$ one can attempt to phase match orthogonally polarized fundamental and SH waves. The index ellipsoid (22.20)

$$\frac{x^2 + y^2}{n_o^2} + \frac{z^2}{n_e^2} = 1 \tag{27.61}$$

Is shown in Fig.27.5a.

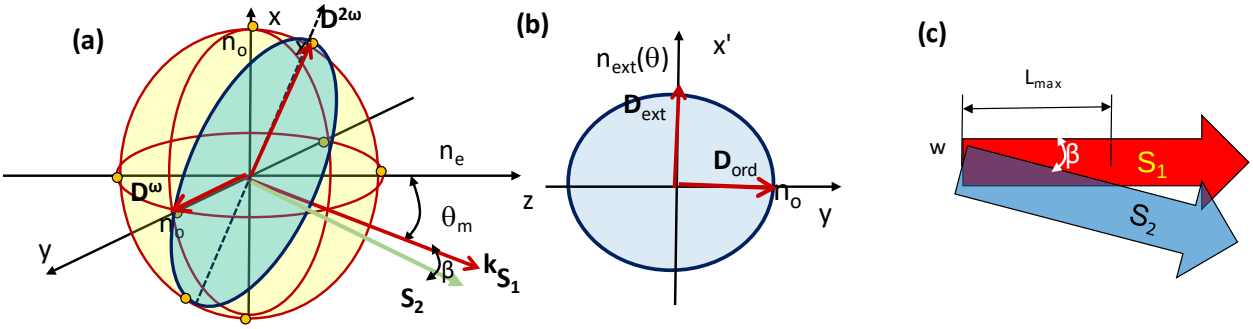

Figure 27.5 (a) Index ellipsoid and geometry of phase-matched SHG (b) Finding extraordinary index (c) Impact of walk-off β.

The fundamental light is propagating at the angle θ_m to the optical axis z and is polarized normal to optical axis. The wavevector $\mathbf{k}$ of SH wave is also directed at the angle θ_m but it is polarized not-orthogonally to the optical axis, hence its Poynting vector $\mathbf{S}_2$ is directed at a walk-off angle β, as discussed in Chapter 22. Now, consider the cross-section of the index ellipsoid with a plane normal to $\mathbf{k}$ shown in Fig.27.5b. The equation for extraordinary index (22.44) is

$$\frac{1}{n_{ext}^2(\theta)} = \frac{\cos^2\theta}{n_o^2} + \frac{\sin^2\theta}{n_e^2} \tag{27.62}$$

Therefore, the phase-matching angle can be determined from

$$n_{2,ext} = \left[\frac{\cos^2\theta_m}{n_{2o}^2} + \frac{\sin^2\theta_m}{n_{2e}^2}\right]^{-1/2} = n_{1,o} \tag{27.63}$$

Solving this equation for the $\cos\theta_m$ we obtain

$$\cos^2\theta_m = \left(\frac{n_{2e}^2 - n_{1,o}^2}{n_{2e}^2 - n_{2o}^2}\right)\frac{n_{2o}^2}{n_{1,o}^2} \tag{27.64}$$

and for our example $\theta_m \approx 50.5^\circ$. Everything looks fine, until one realizes that the walk-off angle is quite large. According to (22.49)

$$\beta = \tan^{-1}\left(\frac{n_{1,o}^2}{n_{2,e}^2}\tan\theta_m\right) - \theta_m \approx 1.7^\circ \tag{27.65}$$

Let us see what it means. If, as shown in Fig.27.5.c the pump beam diameter is $w = 50\mu m$ the two beams will no longer overlap after only $L_{\max} \sim w/\sin\beta = 1.7mm$ which is quite short. This phase-matching is called critical. To avoid walk off one would like to have $\theta_m = 90°$ which would mean $n_{2,e} = n_{1,o}$. That can be achieved by changing temperature – placing the crystal into the oven.

Effective SHG coefficient

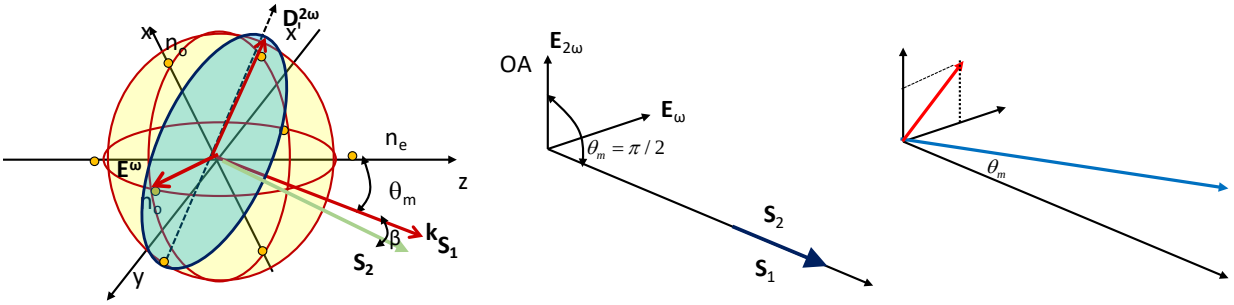

Figure 27.6 (a) How to find effective nonlinear coefficient (b) Non-critical phase matching. (c) Type II phasematching

Since the only non-zero SHG coefficients in KDP are $d_{14}=d_{xzy}$ and $d_{36}=d_{zxy}$,we need the fundamental (pump) wave have two projections and maximize E_xE_y product by choosing the polarization at 45 degrees to axis x as shown in Fig,27.6.a Since the crystal is uniaxial, fundamental wave is is till ordinary and SH is still extraordinary. The effective SHG coefficient is given by (27.45). To start we find the outer product of pump polarization unit vectors

$$\hat{\mathbf{e}}_1 \otimes \hat{\mathbf{e}}_1 = \begin{pmatrix} \frac{1}{\sqrt{2}} & \frac{1}{\sqrt{2}} & 0 \end{pmatrix} \begin{pmatrix} \frac{1}{\sqrt{2}} \\ \frac{1}{\sqrt{2}} \\ 0 \end{pmatrix} = \begin{pmatrix} \frac{1}{2} & \frac{1}{2} & 0 \\ \frac{1}{2} & \frac{1}{2} & 0 \\ 0 & 0 & 0 \end{pmatrix} = \begin{pmatrix} 1/2 \\ 1/2 \\ 0 \\ 0 \\ 0 \\ 1 \end{pmatrix} \tag{27.66}$$

Neglecting walk-off we assume that $\mathbf{E}_2 \parallel \mathbf{D}_2$, then

$$d_{eff} = \hat{\mathbf{e}}_2 \cdot \left[d\hat{\mathbf{e}}_1 \otimes \hat{\mathbf{e}}_1 \right] = \begin{pmatrix} \frac{\cos\theta_m}{\sqrt{2}} \\ \frac{\cos\theta_m}{\sqrt{2}} \\ \sin\theta_m \end{pmatrix} \begin{pmatrix} 0 & 0 & 0 & d_{14} & 0 & 0 \\ 0 & 0 & 0 & 0 & d_{14} & 0 \\ 0 & 0 & 0 & 0 & 0 & d_{36} \end{pmatrix} \begin{pmatrix} 1/2 \\ 1/2 \\ 0 \\ 0 \\ 0 \\ 1 \end{pmatrix} = \begin{pmatrix} \frac{\cos\theta_m}{\sqrt{2}} & \frac{\cos\theta_m}{\sqrt{2}} & \sin\theta_m \end{pmatrix} \begin{pmatrix} 0 \\ 0 \\ d_{36} \end{pmatrix} = d_{36} \sin\theta_m \approx 0.82 d_{36}$$

(27.67)

Acceptance angle

The main problem of critical phase matching is a relatively narrow range of angles (acceptance range) within each phase-matching is preserved. Let us differentiate (27.62) over the angle θ:

$$\frac{d}{d\theta} \frac{1}{n_{ext}^2(\theta)} = \frac{d}{d\theta} \left(\frac{\cos^2\theta}{n_o^2} + \frac{\sin^2\theta}{n_e^2} \right) = \sin 2\theta \frac{n_o^2 - n_e^2}{n_o^2 n_e^2} \tag{27.68}$$

and

$$\frac{d}{d\theta} n_2(\theta) = -\frac{n_2^3(\theta)}{2} \sin 2\theta_m \frac{n_{2o}^2 - n_{2e}^2}{n_{2o}^2 n_{2e}^2} \approx (n_{2e} - n_{2o}) \sin 2\theta_m \tag{27.69}$$

The wave vector mismatch is then proportional to the deviation from phase matching angle

$$\Delta k = 2\frac{\omega}{c} \Delta n_2 = \frac{4\pi}{\lambda} (n_{2e} - n_{2o}) \sin 2\theta_m \times \Delta\theta \tag{27.70}$$

And the coherence length is

$$\Delta k = 2\frac{\omega}{c} \Delta n_2 = \frac{4\pi}{\lambda} (n_{2e} - n_{2o}) \sin 2\theta_m \times \Delta\theta \tag{27.71}$$

The coherence length is

$$L_{coh}(\Delta\theta) = \pi / \Delta k = \frac{\lambda}{4(n_{2e} - n_{2o}) \sin 2\theta_m} \frac{1}{\Delta\theta} = \frac{0.004mm}{\Delta\theta} \tag{27.72}$$

For L=1cm we are constrained to $\Delta\theta \approx 4 \times 10^{-4} \approx 0.023^\circ$ - a rather narrow range of angles. It is hard to collimate the light to that degree. That is why it is important to achieve non-critical phase matching where, as shown in Fig.26.7b the SH is polarized along the optical axis, obviously $\sin(2\theta_m) = 0$ and one has to evaluate the second derivative

$$\frac{d^2}{d\theta^2} n_2(\theta) \approx 2(n_{2e} - n_{2o}) \tag{27.73}$$

So that

$$\Delta k = 2\frac{\omega}{c}\Delta n_2 = \frac{4\pi}{\lambda}(n_{2e} - n_{2o})\frac{(\Delta\theta)^2}{2} \tag{27.74}$$

and

$$L_{coh}(\Delta\theta) = \pi / \Delta k = \frac{\lambda}{2(n_{2e} - n_{2o})}\frac{1}{(\Delta\theta)^2} = \frac{0.007mm}{(\Delta\theta)^2} \tag{27.75}$$

Now for L=1cm we are constrained to $\Delta\theta \approx 0.027 \approx 1.58^\circ$ which is quite an improvement.

Type II phase matching

Sometimes it is more advantageous is to use type II phase matching as shown in Fig. 27.6c. where the fundamental wave contains both ordinary and extraordinary components and in the SH G process one photon of ordinary polarization and one of extraordinary polarization "merge" to create an extraordinary polarized photon at twice the frequency, i.e. $E_{1,o} + E_{1,e} \Rightarrow E_{2,e}$. It is easy to see that phase matching condition is

$$2n_{2,ext}(\theta_m) = n_{1,ext}(\theta_m) + n_{1,o} \tag{27.76}$$

Quasi-Phase Matching (QPM)

Let us take a detailed look at the origin of the periodic oscillations in the amplitude of SH wave. The equation of SHG is (27.48) in which we drop imaginary 1 as an immaterial constant 90 degrees phase shift,

$$\frac{dA_2}{dz} = j\kappa A_1^2 e^{j\Delta kz} \tag{27.77}$$

The solution is

$$A_2(z) = \int_0^z \kappa A_1^2 e^{j\Delta kz_1} dz_1 \tag{27.78}$$

Let us discretize it by splitting the coordinate z into small intervals Δz, then

$$A_{2,n} = A_2(z_n) = \sum_{m=1}^{n} \kappa A_1^2 \Delta z e^{j\Delta km\Delta z} = \sum_{m=1}^{n} \Delta A_2 e^{j\Delta\Phi_m} \tag{27.79}$$

where $\Delta A_2 = \kappa A_1^2 \Delta z$ and $\Delta\Phi_m = m\Delta k\Delta z$. As shown in Fig.27.7a, the increments of amplitude trace an arc as angle $\Delta\Phi_m$ keeps growing. Eventually $m\Delta k\Delta z = \pi$, or $z = \pi / L_{coh}$ SH amplitude reaches maximum

$$A_2(L_{coh}) = \int_0^{L_{coh}} \kappa A_1^2 e^{j\Delta k z_1} dz_1 = \kappa A_1^2 \frac{e^{j\pi} - 1}{j\Delta k} = \frac{2}{\pi} j\kappa A_1^2 L_{coh} \tag{27.80}$$

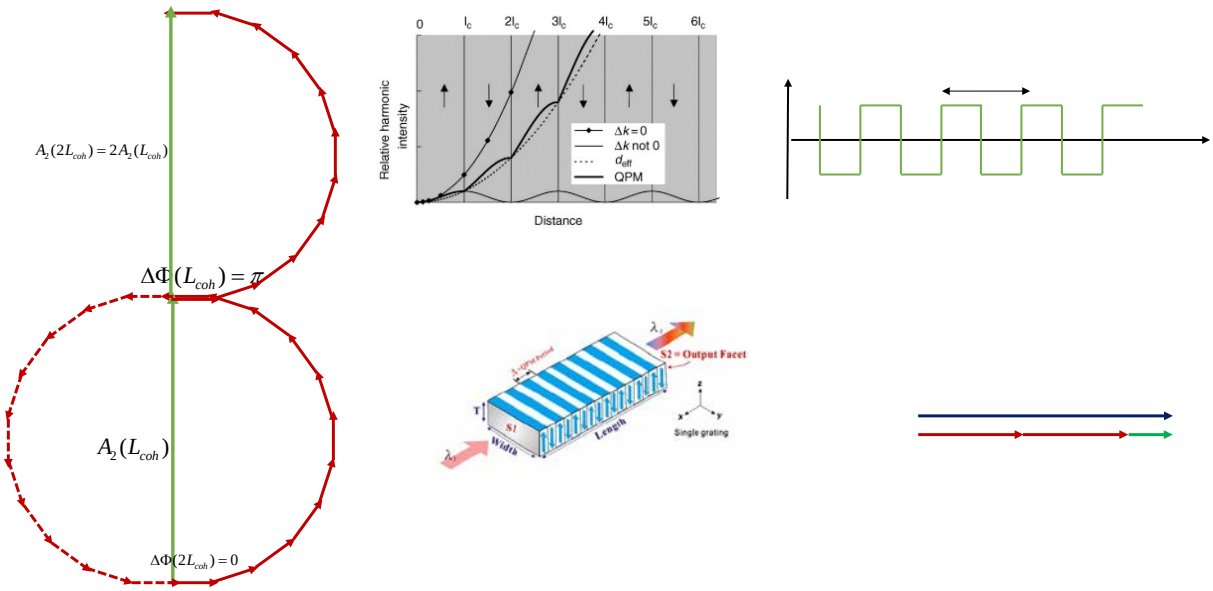

Figure 27.7 (a) Principle of QPM (b) Intensity of SH for the cases of no phasematching, perfect phasematching and QPM (c) PPPLN crystal (d) Profile of SHG coefficient in PPLN (e) Momentum matching in QPM

After that the amplitude of SH starts decreasing and at $z = 2L_{coh}$ competes a full circle. The idea of QPM is simple – since (27.49)

$$\kappa = \frac{2\omega}{n_2 c} d \tag{27.81}$$

And SHG coefficient d has a sign, by reversing this sign, i.e. changing the crystal orientation by 180 degrees we change the sign of κ. This will force the reset of $\Delta\Phi$ back to zero and now the SH amplitude will trace another counterclockwise semi-circle as shown in Fig.27.7.a. Obviously

$$A_2(2L_{coh}) = 2A_2(L_{coh}) = \frac{4}{\pi} j\kappa A_1^2 L_{coh} \tag{27.82}$$

Continuing the periodic reversal, we arrive at

$$A_2(nL_{coh}) = nA_2(L_{coh}) = \frac{2}{\pi} j\kappa A_1^2 nL_{coh}, \tag{27.83}$$

Or, simply

$$A_2(L) = \frac{2}{\pi} j\kappa A_1^2 L \tag{27.84}$$

The same result can of course be obtained by simply solving (27.77) with effective SHG coefficient

$$d_{eff} = \frac{2}{\pi} d \tag{27.85}$$

In Fig.27.7b the intensity of SH vs. distance is shown. For perfect phasematching the increase is parabolic, for no phasematching SH intensity oscillates with a period $2L_c$ and for QPM it also increases albeit not as fast as for perfect phasematching and can be approximated by a parabola with lower slope.

Reversal of the sign of d in $LiNbO_3$ is achieved by periodic poling. $LiNbO_3$ is a ferroelectric material, i..e has permanent dipole moment which can be directed "up" or "down". Applying strong DC field can reverse the permanent polarization and with it the sign of d. Thus one obtains periodically poled lithium niobate or PPLN shown in Fig.27.7.c. What is nice about PPLN is that one can use the largest nonlinear coefficient d_{33}, and since both fundamental and SH are polarized along optical axis, the phasematching is not critical.

In Fig.27.7.d the dependence of SHG coefficient on distance is shown.

$$d(x) = d_{33} F(x) \tag{27.86}$$

where $F(x)$ is a square wave of unit amplitude with period $\Lambda = 2L_{coh} = 2\pi / \Delta k = 7.6\mu m$. One can expand this dependence into Fourier series

$$F(x) = \frac{4}{\pi}\sin(2\pi x / \Lambda) + \frac{4}{\pi}\sin(6\pi x / \Lambda) + ... \tag{27.87}$$

The equation (27.77) then becomes

$$\frac{dA_2}{dx} = j\kappa A_1^2 e^{-j\Delta kx} F(x) = \frac{2}{\pi}\kappa A_1^2 e^{j\Delta kx}\left[e^{j2\pi x/\Lambda} + e^{j6\pi x/\Lambda} + ... + c.c.\right] = \frac{2}{\pi}\kappa A_1^2 e^{j(\Delta k - 2\pi/\Lambda)x} = \kappa_{eff} A_1^2 \tag{27.88}$$

where obviously $\kappa_{eff} = \frac{2}{\pi}\kappa$ and $d_{eff} = \frac{2}{\pi} d_{33}$. One can represent wavevector (momentum) matching by assigning the "nonlinear grating" a wavevector $K_{gr} = 2\pi / \Lambda$, then wavevector matching condition is

$$2\mathbf{k}_\omega + 2\pi / \Lambda = \mathbf{k}_{2\omega} \tag{27.89}$$

As shown in Fig.27.7.e. Obviously, the grating does not need to have 50/50 duty cycle, but 50/50 duty cycle give s\you the largest first Fourier component amplitude $2/\pi$

Three wave interactions

Now we consider a more general case, when three different waves interact via nonlinear coefficient (Fig.27.8)

Three propagating wives are called *signal, idler*, and *pump*.

$$\begin{aligned} E_s(z,t) &= A_s(z)e^{j(k_s z-\omega_s t)} + c.c. \\ E_i(z,t) &= A_i(z)e^{j(k_i z-\omega_i t)} + c.c. \\ E_p(z,t) &= A_p(z)e^{j(k_i z-\omega_i t)} + c.c. \end{aligned} \tag{27.90}$$

Their frequencies are related as

$$\omega_s + \omega_i = \omega_p \tag{27.91}$$

and their wave vectors as

$$k_s + k_i = k_p - \Delta k \tag{27.92}$$

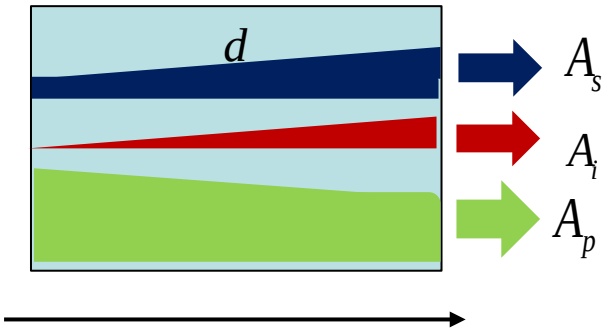

Figure 27.8 Three wave interaction in nonlinear medium

Phase mismatch Δk is small. he nonlinear polarization, according to (27.23) is

$$\begin{aligned} &P^{(2)} = \varepsilon_0 d_{eff}(E_s + E_i + E_p)^2 = \\ &= 2\varepsilon_o d_{eff} A_s A_i e^{j[(k_s+k_i)z-\omega_p t]} + 2\varepsilon_o d_{eff} A_p A_i^* e^{j[(k_p-k_i)z-\omega_s t]} + 2\varepsilon_o d_{eff} A_p A_s^* e^{j[(k_p-k_s)z-\omega_i t]} \end{aligned} \tag{27.93}$$

We neglect SH terms because SHG processes have very large mismatch. Next we substitute (27.93) into the wave equation, neglect second derivatives, and equate the terms with the same temporal dependence to obtain three coupled differential equations

$$
\begin{aligned}
2jk_s \frac{dA_s}{dz} e^{j(k_s z-\omega_s t)} &= -2\frac{\omega_s^2}{c^2} d_{eff} A_p A_i^* e^{j[(k_p-k_i)z-\omega_s t]} \\
2jk_i \frac{dA_i}{dz} e^{j(k_i z-\omega_i t)} &= -2\frac{\omega_i^2}{c^2} d_{eff} A_p A_s^* e^{j[(k_p-k_s)z-\omega_i t]} \\
2jk_p \frac{dA_s}{dz} e^{j(k_s z-\omega_s t)} &= -2\frac{\omega_p^2}{c^2} d_{eff} A_s A_i e^{j[(k_s+k_i)z-\omega_p t]}
\end{aligned}
\tag{27.94}
$$

or

$$
\begin{aligned}
\frac{dA_s}{dz} &= j\frac{\omega_s}{n_s c} d_{eff} A_p A_i^* e^{j\Delta kz} \\
\frac{dA_i}{dz} &= j\frac{\omega_s}{n_i c} d_{eff} A_p A_s^* e^{j\Delta kz} \\
\frac{dA_p}{dz} &= j\frac{\omega_p}{n_p c} d_{eff} A_s A_i e^{-j\Delta kz}
\end{aligned}
\tag{27.95}
$$

Next we get rid of exponentials by introducing new phase-shifted variables for signal and idler

$$
A_{s,i} = A_{s,i}^{'} e^{j\Delta kz/2} \tag{27.96}
$$

And substituting them into (27.95)to obtain

$$
\begin{aligned}
\frac{dA_s^{'}}{dz} + j\frac{\Delta k}{2} A_s^{'} &= j\frac{\omega_s}{n_s c} d_{eff} A_p A_i^{'*} \\
\frac{dA_i^{'}}{dz} + j\frac{\Delta k}{2} A_i^{'} &= j\frac{\omega_i}{n_i c} d_{eff} A_p A_s^{'*} \\
\frac{dA_p}{dz} &= j\frac{\omega_p}{n_i c} d_{eff} A_s^{'} A_i^{'}
\end{aligned}
\tag{27.97}
$$

Next, introduce the power densities (27.53)

$$
S_m = \frac{2n_m \left|A_m\right|^2}{\eta_0}, \; m = s, i, p \tag{27.98}
$$

and photon flux densities – number of photons per second per unit area

$$
N_m = \frac{S_m}{\hbar\omega_m} = \frac{2n_m \left|A_m\right|^2}{\eta_0 \hbar\omega_m} \tag{27.99}
$$

Finally, introduce the normalized amplitudes a_m as

$$A_m^{'} = \sqrt{\frac{\eta_0 \hbar \omega_m}{2n_m}} a_m;\ N_m = |\, a_m \,|^2 \tag{27.100}$$

Note that units of a_m are $cm^{-1}s^{-1/2}$ Substitute it into (27.97) and obtain

$$\begin{aligned} &\frac{da_s}{dz} + j\frac{\Delta k}{2} a_s = j\kappa a_p a_i^* \\ &\frac{da_i}{dz} + j\frac{\Delta k}{2} a_i = j\kappa a_p a_s^* \\ &\frac{da_p}{dz} = j\kappa a_s a_i \end{aligned} \tag{27.101}$$

Where the coupling coefficient is now

$$\kappa = \frac{d_{eff}}{c}\sqrt{\frac{\hbar \eta_0 \omega_s \omega_i \omega_p}{2n_s n_i n_p}}\ (s^{1/2}) \tag{27.102}$$

Let us find change in photon fluxes

$$\begin{aligned} &\frac{dN_{s,i}}{dz} = a_{s,i}^* \frac{da_{s,i}}{dz} + c.c. = j\kappa a_p a_i^* a_s^* - j\kappa a_p^* a_i\, a_s \\ &\frac{dN_p}{dz} = a_p^* \frac{da_p}{dt} + c.c. = j\kappa a_p^* a_i\, a_s - j\kappa a_p a_i^* a_s^* = -\frac{dN_{s,i}}{dt} \end{aligned} \tag{27.103}$$

This shows quantum character of interaction – the signal and idler photon combine into a single pump photon , and, vice versa, pump photon splits into signal and idler photons. The numbers are conserved and we have Manley-Rowe relation

$$\Delta N_s = \Delta N_i = -\Delta N_p \tag{27.104}$$

which is also a power conservation

$$\Delta(S_s + S_i + S_p) = \hbar\omega_s \Delta N_s + \hbar\omega_i \Delta N_i - \hbar\omega_p \Delta N_p = \Delta N_s \hbar(\omega_s + \omega_i - \omega_p) = 0; \tag{27.105}$$

SHG with pump depletion

For SHG case we introduce a new notation

$$\begin{aligned} &A_s = A_1 \quad \omega_s = \omega_i = \omega \\ &A_p = A_2 \quad \omega_p = 2\omega \end{aligned} \tag{27.106}$$

The equations (27.95) are now

$$\frac{dA_1}{dz} = j\frac{\omega}{n_1 c} d_{eff} A_2 A_1^* e^{j\Delta kz}$$
$$\frac{dA_2}{dz} = j\frac{2\omega}{n_2 c}\frac{1}{2} d_{eff} A_1^2 e^{-j\Delta kz} \quad (27.107)$$

And introducing

$$A_1 = A_1' e^{j\Delta kz/4}$$
$$A_2 = jA_2' e^{-j\Delta kz/2} \quad (27.108)$$

and using (27.100) we obtain

$$\frac{da_1}{dz} + j\frac{\Delta k}{4} a_1 = -\kappa a_2 a_1^*$$
$$\frac{da_2}{dz} - j\frac{\Delta k}{2} a_2 = \frac{1}{2}\kappa a_1^2 \quad (27.109)$$

where

$$\kappa = \frac{d_{eff}\omega}{c}\sqrt{\frac{\hbar \eta_0 \omega}{n_1^2 n_2}} \quad (27.110)$$

Let us consider the case of perfect phase matching, $\Delta k = 0$

$$\frac{da_1}{dz} = -\kappa a_2 a_1^*$$
$$\frac{da_2}{dz} = \frac{1}{2}\kappa a_1^2 \quad (27.111)$$

It is easy to see that one can have a solution in which both amplitudes are real, i.e.

$$\frac{da_1}{dz} = -\kappa a_2 a_1$$
$$\frac{da_2}{dz} = \frac{1}{2}\kappa a_1^2 \quad (27.112)$$

For the photon flux densities we have

$$\frac{da_1^2}{dz} = -2\kappa a_2 a_1^2$$
$$\frac{da_2^2}{dz} = \kappa a_2 a_1^2 \quad (27.113)$$

i.e. $\Delta N_2 = -\frac{1}{2}\Delta N_1$, meaning that two fundamental photons combine to create SH photon and that one in turn splits into two fundamental photons. The power is conserved, i.e.

$$a_1^2 + 2a_2^2 = a_1^2(0) = N_{1,0} \tag{27.114}$$

where $a_1^2(0) = N_{1,0}$ is the input fundamental photon flux. Expressing $a_1^2 = N_{1,0} - 2a_2^2$ and substituting into the second equation in (27.112) we obtain

$$\frac{da_2}{dz} = \frac{1}{2}\kappa(N_{1,0} - 2a_2^2) \tag{27.115}$$

To solve it we note that $\frac{d}{dx}\tanh(x) = 1 - \tanh^2(x)$ so we can try $a_2 = C\tanh(\gamma z)$ where both gain coefficient γ and C need to be found from boundary conditions. Substitution yields

$$\frac{da_2}{dz} + \kappa a_2^2 = C\gamma[1 - \tanh^2(\gamma z)] + \kappa C^2 \tanh^2(\gamma z) = \frac{1}{2}\kappa N_{1,0} \tag{27.116}$$

The terms with hyperbolic tangent must be cancelled, so $\gamma = C\kappa$ and then it follows that $C\gamma = \frac{1}{2}\kappa N_{1,0}$. Then

$$\begin{aligned} &\gamma^2 = \frac{1}{2}\kappa^2 N_{1,0};\ \gamma = \kappa\sqrt{\frac{N_{1,0}}{2}} \\ &C = \frac{\gamma}{\kappa} = \sqrt{\frac{N_{1,0}}{2}} \end{aligned} \tag{27.117}$$

and we obtain

$$N_2(z) = a_2^2(z) = \frac{N_{1,0}}{2}\tanh^2\left(\kappa\sqrt{\frac{N_{1,0}}{2}}z\right) \tag{27.118}$$

Which makes perfect sense that the output photon flux density saturates saturates at exactly one half of the fundamental input photon flux density-100% conversion efficiency For the output power density we have

$$S_{out} = 2\hbar\omega N_2(L) = a_2^2(L) = S_{in}\tanh^2\left(\frac{d_{eff}\omega}{c}\sqrt{\frac{\eta_0 S_{in}}{2n_1^2 n_2}}L\right) \tag{27.119}$$

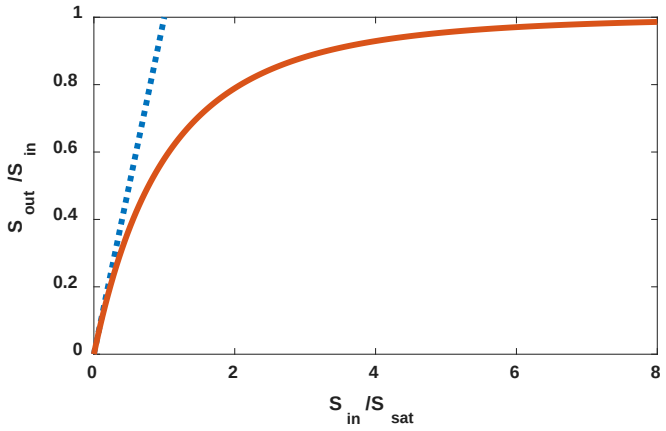

Figure 27.9 SHG with pump power depletion

Introduce saturation input photon flux density as

$$S_{sat} = \frac{2n_1^2 n_2 c^2 \eta_0}{\omega^2 d_{eff}^2 L^2} \tag{27.120}$$

Then we have

$$\frac{S_{out}}{S_{in}} = \tanh^2\left(\sqrt{\frac{S_{in}}{S_{sat}}}\right) \tag{27.121}$$

As shown in Fig.27.9 power efficiency first increases linearly with input power but then indeed saturates at 100%

Frequency upconversion (Sum Frequency Generation)

What if We want to convert light of Imid-R frequency ω_1 into the light of visible frequency ω_3 with the help of near IR pump $\omega_2 = \omega_3 - \omega_1$. This way IR image becomes a visible image as shown in Fig.27.10.a The relation between the wavevectors is shown in Fig.27.910b Assume that pump E_2 is not depleted and $\Delta k=0$. We also assume that the amplitude A_1 is real Then we have from (27.101)

$$\begin{aligned} &\frac{da_1}{dz} = j\kappa a_3 a_2^* \\ &a_2 \approx a_2(0) = a_2^* \ (real) \\ &\frac{da_3}{dz} = j\kappa a_1 a_2 \end{aligned} \tag{27.122}$$

And introducing $a_3 = ja_3'$ and then just dropping the prime (phase is not important) we obtain

$$\frac{da_1}{dz} = -\gamma a_3$$
$$\frac{da_3}{dz} = \gamma a_1 \tag{27.123}$$

where the gain coefficient is

$$\gamma = \kappa a_2 = \frac{d_{eff}}{c}\sqrt{\frac{\hbar\eta_0\omega_1\omega_2\omega_3}{2n_1n_2n_3}}\sqrt{\frac{S_2}{\hbar\omega_2}} = \frac{d_{eff}}{c}\sqrt{\frac{\eta_0\omega_1\omega_3}{2n_1n_2n_3}S_2} \tag{27.124}$$

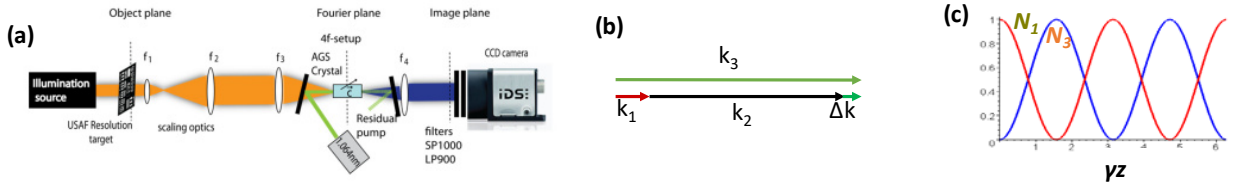

Figure 27.10 (a) upconversion of mid IR light to viible with the help of near IR pump. (b) wavevector matching (c) Coupling between input and upconverted photons

Solution of (27.123) is well-known combination of sine and cosine

$$a_1(z) = a_1(0)\cos\gamma z + C\sin\gamma z$$
$$a_3(z) = -\frac{1}{\gamma}\frac{da_1(z)}{dz} = a_1(0)\sin\gamma z - C\cos\gamma z \tag{27.125}$$

Easy to see that $C = -a_3(0)$ and

$$a_1(z) = a_1(0)\cos\gamma z - a_3(0)\sin\gamma z$$
$$a_3(z) = a_1(0)\sin\gamma z + a_3(0)\cos\gamma z \tag{27.126}$$

Typically, $a_3(0) = 0$ **,**and we can write

$$N_3(z) = a_3^2 = N_{1,0}\sin^2\gamma z$$
$$N_1(z) = a_1^2 = N_{1,0}\cos^2\gamma z \tag{27.127}$$

as shown in Fig.27.10.c. The power couples back and forth between input and upconverted output and 100% conversion is achieved at L=π/2γ.

Parametric down conversion and amplification (Difference Frequency Generation)

No we consider the case of three-wave interaction of Fig.27.8 and Eqs.(27.101) under the condition that the strong pump causes DFG and amplification of both idler and idler. The equations are

$$\begin{aligned}
&\frac{da_s}{dz} + j\frac{\Delta k}{2}a_s = j\kappa a_p a_i^* - \frac{1}{2}\alpha a_s \\
&\frac{da_i}{dz} + j\frac{\Delta k}{2}a_i = j\kappa a_p a_s^* - \frac{1}{2}\alpha a_i \\
&\frac{da_p}{dz} = j\kappa a_s a_i
\end{aligned} \tag{27.128}$$

where α is the loss per unit length (1/2 is because the loss α is for power and equations are for the field amplitude). We consider the case of undepleted pump and introduce the power gain coefficient

$$\gamma = 2\kappa a_p \tag{27.129}$$

. Then (27.128) becomes

$$\begin{aligned}
&\frac{da_s}{dz} + j\frac{\Delta k}{2}a_s + \frac{1}{2}\alpha a_s = j\frac{\gamma}{2}a_i^* \\
&\frac{da_i^*}{dz} - j\frac{\Delta k}{2}a_i^* + \frac{1}{2}\alpha a_i^* = -j\frac{\gamma}{2}a_s
\end{aligned} \tag{27.130}$$

(note that the second equation is written for the complex conjugate of the idler amplitude). Comparing with (27.123) we can see that the terms on r.h.s. now have opposite signs, hence rather than sine and cosine solution one shall expect the hyperbolic sine and cosine. So we shall look for $a_{s,i} \sim \exp(\frac{1}{2}gz)$ and substitute it into (27.130)to get

$$\begin{aligned}
&\left(\frac{g}{2} + \frac{\alpha}{2} + j\frac{\Delta k}{2}\right)a_s - j\frac{\gamma}{2}a_i^* = 0 \\
&\left(\frac{g}{2} + \frac{\alpha}{2} - j\frac{\Delta k}{2}\right)a_i^* + j\frac{\gamma}{2}a_s = 0
\end{aligned} \tag{27.131}$$

or in matrix form

$$\begin{pmatrix} g + \alpha + j\Delta k & -j\gamma \\ j\gamma & g + \alpha - j\Delta k \end{pmatrix}\begin{pmatrix} a_s \\ a_i^* \end{pmatrix} = 0 \tag{27.132}$$

The nontrivial solution exists only if the determinant is zero and we obtain characteristic equation

$$(g + \alpha)^2 + \Delta k^2 = \gamma^2 \tag{27.133}$$

Having solution

$$g_{1,2} = \pm\sqrt{\gamma^2 - \Delta k^2} - \alpha \tag{27.134}$$

It is easy to see that as long as $\gamma > \Delta k$ the solution is a real exponential, and then, if $\gamma^2 > \Delta k^2 + \alpha^2$ the solution is actually exponentially increasing, i.e. we have gain for both idler and signal. If we assume perfect phasematching $\Delta k = 0$, then $g_{1,2} = \pm\gamma - \alpha$ and we have

$$a_s(z) = \left[C_1 \cosh\frac{\gamma}{2} z + C_2 \sinh\frac{\gamma}{2} z \right] e^{-\frac{\alpha}{2}z}$$
$$a_i^*(z) = -j\left[C_2 \cosh\frac{\gamma}{2} z + C_1 \sinh\frac{\gamma}{2} z \right] e^{-\frac{\alpha}{2}z} \quad (27.135)$$

From the boundary conditions at z=0

$$C_1 = a_s(0)$$
$$C_2 = j a_i^*(0) \quad (27.136)$$

and therefore

$$a_s(z) = \left[a_s(0) \cosh\frac{\gamma}{2} z + j a_i^*(0) \sinh\frac{\gamma}{2} z \right] e^{-\frac{\alpha}{2}z}$$
$$a_i^*(z) = \left[a_i^*(0) \cosh\frac{\gamma}{2} z - j a_s(0) \sinh\frac{\gamma}{2} z \right] e^{-\frac{\alpha}{2}z} \quad (27.137)$$

For photon flux densities we obtain

$$N_s(z) = |a_s(z)|^2 = \left[N_s(0) \cosh^2\frac{\gamma}{2} z + N_i(0) \sinh^2\frac{\gamma}{2} z \right] e^{-\alpha z}$$
$$N_i(z) = |a_i(z)|^2 = \left[N_i(0) \cosh^2\frac{\gamma}{2} z + N_s(0) \sinh^2\frac{\gamma}{2} z \right] e^{-\alpha z} \quad (27.138)$$

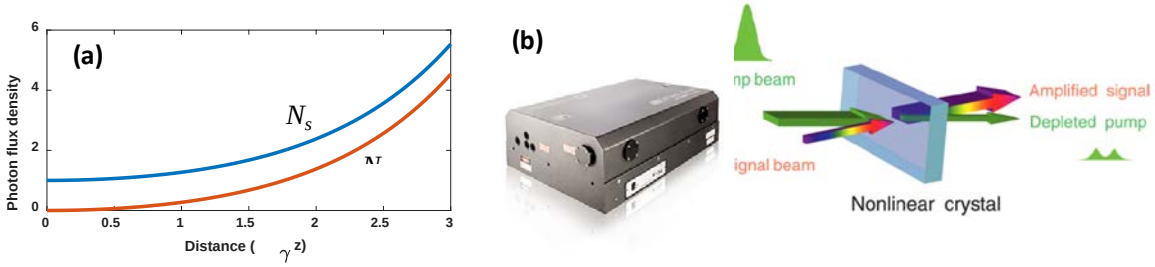

Figure 27.11. (a) Signal and Idler photon fluxes vs length (b) Optical Paramterc Amplifier

The results are shown in in Fig. 29.11 for the most common case when $N_i(0) = 0$. Note that both signal and idler get amplified (as long as $\gamma > \alpha$). Also note that

$$N_s(z) - N_i(z) = [N_s(0) - N_i(0)] e^{-\alpha z} \quad (27.139)$$

Therefore, discounting the attenuation, the difference between the numbers of signal and idler photons does not change, which is, of course, expected as two photons can only appear simultaneously. Also note that for $\gamma z >> 1$ sinh and cosh can be approximated as exponentials and

$$N_s(z) \approx N_i(z) \approx \left[N_s(0) + N_i(0) \right] e^{(\gamma-\alpha)z} \quad (27.140)$$

The optical parametric amplifier is shown in Fig.27.11b. Let us estimate the parametric gain. According to (27.102) and (27.129)

$$\gamma = 2\kappa a_p = 2\frac{d_{eff}}{c}\sqrt{\frac{\hbar\eta_0\omega_s\omega_i\omega_p}{2n_s n_i n_p}}\sqrt{\frac{S_p}{\hbar\omega_p}} = \frac{d_{eff}}{c}\sqrt{\frac{2\eta_0\omega_s\omega_i}{n_s n_i n_p}S_p} = 2\pi d_{eff}\sqrt{\frac{2\eta_0 S_p}{\lambda_s\lambda_i n_s n_i n_p}} \quad (27.141)$$

Consider example of PPLN with $d_{eff} = 20\,pm/V$, $\lambda_{s,i} \approx 1\mu m$, $S_p = 1MW/cm^2$ the gain is about $\gamma \sim 1cm^{-1}$, i.e. rather small. This gain, however is sufficient to achieve self-sustained oscillations on the signal and idler frequencies by introducing optical feedback, i.e. Fabry-Perot resonator as shown in Fig. 27.12.

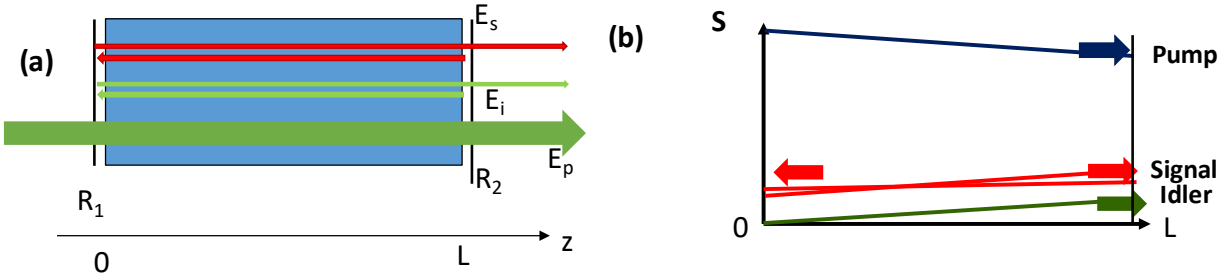

Figure 27.12 (a) scheme of a double-resonant OPO (b) photon fluxes in single-resonant OPO

Optical parametric oscillator (OPO)

In OPO, just like in a laser, there si no input on either signal or idler frequencies – the radiation arises from spontaneous emission (also known as noise), just like in any other oscillator, be it a laser or electronic oscillator. Let us write the relation between signal and idler signals at z=0 and z=L (27.137) in a matrix form

$$\begin{pmatrix} a_s(L) \\ a_i^*(L) \end{pmatrix} = e^{-\frac{\alpha}{2}L}\begin{pmatrix} \cosh\frac{\gamma}{2}L & j\sinh\frac{\gamma}{2}L \\ -j\sinh\frac{\gamma}{2}L & \cosh\frac{\gamma}{2}L \end{pmatrix}\begin{pmatrix} a_s(0) \\ a_i^*(0) \end{pmatrix} \quad (27.142)$$

Now, two mirrors have reflection coefficients for amplitudes $r_{1,2}$ for signal and idler – in matrix form they are diagonal

$$r_{1(2)} = \begin{pmatrix} r_{1(2)s} & 0 \\ 0 & r_{1(2)i} \end{pmatrix} \quad (27.143)$$

Then one can right the expression for the amplitudes of signal and idler after one round trip, noting that parametric amplification takes place only when the light propagates forward because in backward directions the phasematching is absent.

$$\begin{pmatrix} a_s(0) \\ a_i^*(0) \end{pmatrix} = r_1 r_2 \begin{pmatrix} a_s(L) \\ a_i^*(L) \end{pmatrix} e^{-\frac{\alpha}{2}L} = r_1 r_2 e^{-\alpha L} \begin{pmatrix} \cosh\frac{\gamma}{2}L & j\sinh\frac{\gamma}{2}L \\ -j\sinh\frac{\gamma}{2}L & \cosh\frac{\gamma}{2}L \end{pmatrix} \begin{pmatrix} a_s(0) \\ a_i^*(0) \end{pmatrix} \tag{27.144}$$

Now, if after one round trip the fields are the same then one has a steady oscillation condition and the gain is the threshold gain γ_t. Multiply l.h.s. of (27.144) by unity matrix

$$\begin{pmatrix} 1 & 0 \\ 0 & 1 \end{pmatrix} \begin{pmatrix} a_s(0) \\ a_i^*(0) \end{pmatrix} = \begin{pmatrix} r_{1s} & 0 \\ 0 & r_{1i} \end{pmatrix} \begin{pmatrix} r_{2s} & 0 \\ 0 & r_{2i} \end{pmatrix} e^{-\alpha L} \begin{pmatrix} \cosh\frac{\gamma_t}{2}L & j\sinh\frac{\gamma_t}{2}L \\ -j\sinh\frac{\gamma_t}{2}L & \cosh\frac{\gamma_t}{2}L \end{pmatrix} \begin{pmatrix} a_s(0) \\ a_i^*(0) \end{pmatrix} \tag{27.145}$$

and re-formulate it as

$$\begin{pmatrix} 1 - r_{1s}r_{2s}e^{-\alpha L}\cosh\frac{\gamma_t}{2}L & jr_{1s}r_{2s}e^{-\alpha L}\sinh\frac{\gamma_t}{2}L \\ -jr_{1i}r_{2i}e^{-\alpha L}\sinh\frac{\gamma_t}{2}L & 1 - r_{1i}r_{2i}e^{-\alpha L}\cosh\frac{\gamma_t}{2}L \end{pmatrix} \begin{pmatrix} a_s(0) \\ a_i^*(0) \end{pmatrix} = 0 \tag{27.146}$$

As usual, we have a situation where non-trivial solution exists only if determinant of matrix is zero, so we end up with a characteristic equation

$$1 - e^{-\alpha L}(r_{1s}r_{2s} + r_{1i}r_{2i})\cosh\frac{\gamma_t}{2}L + r_{1i}r_{2i}r_{1s}r_{2s}e^{-2\alpha L} = 0 \tag{27.147}$$

Since the gain coefficient is typically small, use the approximation $\cosh\frac{\gamma_t}{2}L \approx 1 + \frac{1}{8}\gamma_t^2 L^2$ in (27.147)

$$1 - r_{1s}r_{2s}e^{-\alpha L} - r_{1i}r_{2i}e^{-\alpha L} + r_{1i}r_{2i}r_{1s}r_{2s}e^{-2\alpha L} - (r_{1s}r_{2s}e^{-\alpha L} + r_{1i}r_{2i}e^{-\alpha L})\frac{\gamma_t^2 L^2}{8} = 0 \tag{27.148}$$

and then

$$\gamma_t^2 L^2 = \frac{8(1 - r_{1s}r_{2s}e^{-\alpha L})(1 - r_{1i}r_{2i}e^{-\alpha L})}{r_{1s}r_{2s}e^{-\alpha L} + r_{1i}r_{2i}e^{-\alpha L}} \tag{27.149}$$

is the threshold condition. Now consider the situation of double-resonant OPO when Fabry-Perot cavity is resonant at both signal nd idler frequencies with high reflectivities, so that the round trip loss is very small

$$1 - r_{1s(i)}r_{2s(i)}e^{-\alpha L} << 1 \tag{27.150}$$

Then denominator of (27.149) is close to 2 and the threshold gain is

$$\gamma_t L = 2\sqrt{(1 - r_{1s}r_{2s}e^{-\alpha L})(1 - r_{1i}r_{2i}e^{-\alpha L})} \tag{27.151}$$

Just to gain the scale, assume reasonable round trip loss of 10%, i..e $r_{1s(i)}r_{2s(i)}e^{-\alpha L}=0.9$, then one requires $\gamma_t L=0.2$. Let us find the threshold pump power density, according to (27.141),

$$S_{pt}=\frac{\lambda_s\lambda_i n_s n_i n_p}{8\pi^2\eta_0 d_{eff}^2}\gamma_t \tag{27.152}$$

Using the same PPLN example, $d_{eff}=20\,pm/V$, $\lambda_{s,i}\approx 1\mu m$, $L=2cm$ we obtain $S_{pt}\sim 90kW/cm^2$. Threshold is low but the operation is very unstable as it is difficult to maintain resonance at two separate wavelengths simultaneously.

For this reason, a single-resonant OPO is typically used with resonance only at signal frequency and low reflectivity at idler frequency, i.e. $r_{1s}r_{2s}e^{-\alpha L}\sim 1$, $r_{1i}r_{2i}e^{-\alpha L}\sim 0$. Now the denominator in (27.149) is roughly 1 and threshold gain is

$$\gamma_t L=2\sqrt{2(1-r_{1s}r_{2s}e^{-\alpha L})} \tag{27.153}$$

Now if $r_{1s}r_{2s}e^{-\alpha L}=0.9$ the threshold gain is $\gamma_t L=0.9$ and the threshold pump power density in the same PPLN crystal is $S_{pt}\sim 400kW/cm^2$ - which is higher than in double resonant OPO but is still reasonable. The single resonant OPO is quite stable and robust. As shown in Fig.27.12. b the idler in the single OPO cavity starts from 0 on the left.

OPO conversion efficiency

So, we have determined the threshold of OPO, but what kind of output power and conversion efficiency can it provide? To determine it, first, let us make some approximation. Since the round trip gain is relatively small, we assume that the circulating flow of signal photons is roughly constant. We also neglect loss α. At the same time, we cannot neglect the pump depletion anymore, so, from (27.128) we get

$$\begin{aligned} a_s &= const\ \ (real)\\ \frac{da_i}{dz} &= j\kappa a_p a_s\\ \frac{da_p}{dz} &= j\kappa a_s a_i \end{aligned} \tag{27.154}$$

This equation has obvious sine/cosine solution. The boundary conditions are

$$\begin{aligned} a_p(0) &= N_{p,in}^{1/2}\\ a_i(0) &= 0 \end{aligned} \tag{27.155}$$

And the solution is then

$$N_i(L) = a_i^2(L) = N_{p,in}\sin^2\kappa a_s L$$
$$N_p(L) = a_1^2 = N_{p,in}\cos^2\kappa a_s L \tag{27.156}$$

Since the idler is not reflected all idler photons exit the OPO, i.e.

$$N_{i,out} = N_i(L) = N_{p,in}\sin^2\left(\kappa a_s L\right) \tag{27.157}$$

Let us now find the flux of signal photons exiting the cavity (on both ends)

$$N_{s,out} = a_s^2\left[(1-r_{1s}^2)+(1-r_{2s}^2)\right] = 2a_s^2\left(1-\frac{r_{1s}^2+r_{2s}^2}{2}\right) \approx 2a_s^2\left(1-r_{1s}r_{2s}\right) \tag{27.158}$$

where we used $r_{1s} \sim r_{2s} \sim 1$. But we also know that signal and idler photons are created and decayed in equal numbers, hence $N_{i,out} = N_{s,out}$ and we can write

$$N_{p,in}\sin^2\left(\kappa a_s L\right) = 2a_s^2\left(1-r_{1s}r_{2s}\right) \tag{27.159}$$

Dived both sides of (27.159) by $N_{p,in}(\kappa a_s L)^2$ and obtain

$$\frac{\sin^2\left(\kappa a_s L\right)}{\left(\kappa a_s L\right)^2} = \frac{2\left(1-r_{1s}r_{2s}\right)}{N_{p,in}\kappa^2 L^2} \tag{27.160}$$

Now we know that threshold gain is (27.153)

$$\gamma_t L = 2\sqrt{2(1-r_{1s}r_{2s})} \tag{27.161}$$

And also that at threshold according to (27.129)

$$\gamma_t = 2\kappa a_{pt} = 2\kappa\sqrt{N_{pt}} \tag{27.162}$$

where N_{pt} is threshold photon flux. It follows then that

$$\gamma_t^2 = 4\kappa^2 N_{pt} = 8(1-r_{1s}r_{2s})/L^2 \tag{27.163}$$

and $N_{pt} = 2(1-r_{1s}r_{2s})/\kappa^2 L^2$, then we obtain from (27.160)

$$\frac{\sin^2\left(\kappa a_s L\right)}{\left(\kappa a_s L\right)^2} = \frac{N_{pt}}{N_{p,in}} = \frac{S_{pt}}{S_{p,in}} \tag{27.164}$$

Therefore, once if we know the input pump power relative to the threshold, we can find $x = \kappa a_s L$, for example graphically as shown in Fig. 27.13. And then, according to (27.157) we find the photon conversion efficiency

$$\eta = \frac{N_{i,out}}{N_{p,in}} = \sin^2 x \tag{27.165}$$

As also graphically shown in Fig.21.13. As one can see, very high conversion efficiencies are possible, in practice 80% has been achieved.

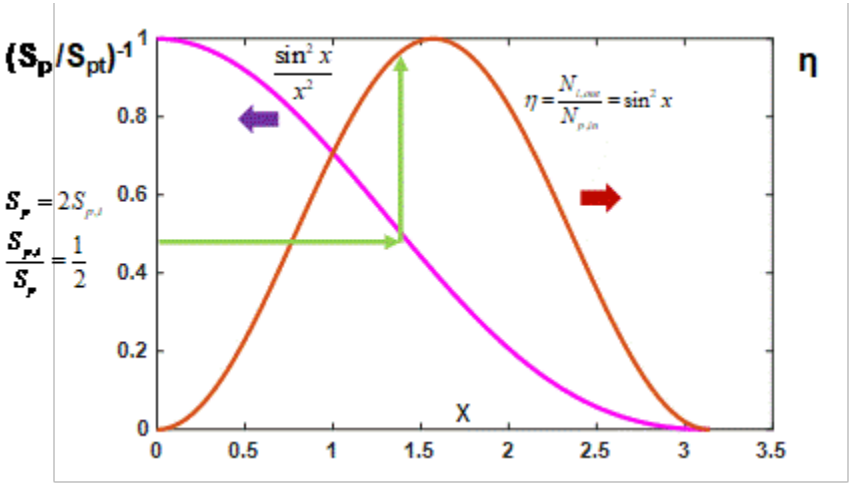

Figure 27.13 – Estimating OPO photon conversion efficiency

OPO tuning

The most important characteristics of OPO is the ability to tune the wavelengths of signal and idler over a wide range while keeping the same pump wavelength. Let us write the phase mismatch (27.92) $\Delta\mathbf{k} = \mathbf{k}_s + \mathbf{k}_i - \mathbf{k}_p$ and assume the phase matching is achieved for the degenerate case $\omega_s = \omega_i = \omega_p / 2$

$$c\Delta k_0 = 2n\left(\omega_p / 2\right)\cdot\frac{\omega_p}{2} - n(\omega_p)\cdot\omega_p = 0 \tag{27.166}$$

What if change some parameter x, say angle, temperature, or period of QPM structure, the mismatch will also change as

$$\Delta k(x) \approx \Delta k_0 + \frac{\partial \Delta k}{\partial x}(x - x_m) = \frac{\partial \Delta k}{\partial x}(x - x_m) \tag{27.167}$$

For example, if we change angle, i.e. $x = \theta$, as shown in Fig.27.14 a then, according to (27.71)

$$\Delta k(\theta) = \frac{4\pi}{\lambda}(n_{p,e} - n_{p,o})\sin 2\theta_m \times (\theta - \theta_m) \tag{27.168}$$

To keep the phase-matching condition the frequencies of signal and idler will have to change, obviously by equal amount

$$\omega_s = \omega_p / 2 + \Delta\omega,\ \ \omega_i = \omega_p / 2 - \Delta\omega \tag{27.169}$$

Then

$$\Delta k(x,\Delta\omega) = k(\omega_p/2) + \frac{\partial k}{\partial \omega}\Delta\omega + \frac{1}{2}\frac{\partial^2 k}{\partial \omega^2}\Delta\omega^2 + k(\omega_p/2) - \frac{\partial k}{\partial \omega}\Delta\omega + \frac{1}{2}\frac{\partial^2 k}{\partial \omega^2}\Delta\omega^2 - k(\omega_p) + \frac{\partial \Delta k}{\partial x}(x - x_m) = 0 \tag{27.170}$$

or introducing group velocity dispersion $\beta_2 = \partial^2 k / \partial \omega^2$ (Chapter 21) we obtain

$$\beta_2 \Delta\omega^2 = \frac{\partial \Delta k}{\partial x}(x_m - x) \tag{27.171}$$

Now we obtain the values of signal and idler frequencies,

$$\omega_{s,i}(x) = \frac{\omega_p}{2} \pm \sqrt{A(x_0 - x)} \tag{27.172}$$

, where

$$A = \frac{\frac{\partial \Delta k}{\partial x}}{\beta_2} \tag{27.173}$$

The tuning curve is shown in Fig.27.14b Tuning range increases with decrease in group velocity dispersion. Note that presence of the square root in (27.172) indicates that parameter x can be varied in one direction, depending the sign of A. For the example where x is the angle,

$$\omega_{s,i}(\theta) = \frac{\omega_p}{2} \pm \sqrt{\frac{4\pi}{\lambda\beta_2}(n_{p,e} - n_{p,o})\sin 2\theta_m \cdot (\theta_m - \theta)} \tag{27.174}$$

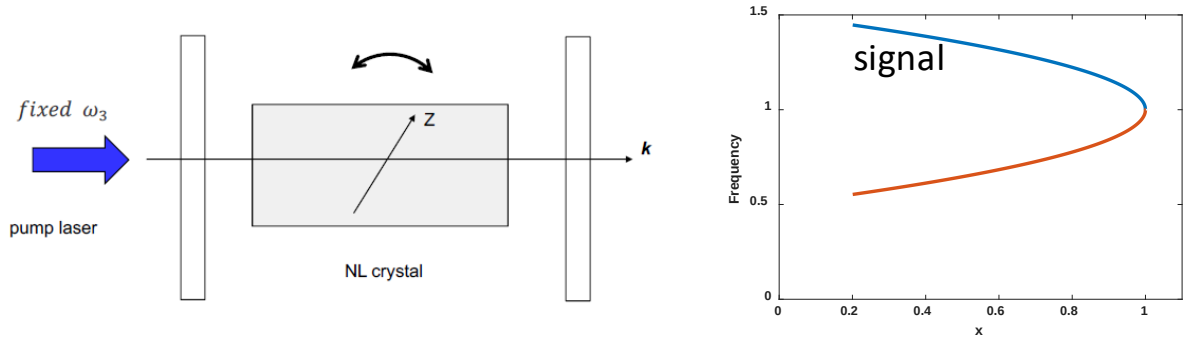

Figure 27.14 (a) angle tuning of OPO (b) OPO tuning curve

A few examples of OPO tuning are shown below. In 27.15.a it is for $LiNbO_3$ crystal pumped by 1060nm (Nd:YAG laser) – changing angle by a few degrees results in tuning OPO output(s) between 1.5 and 4.5µm. In Fig.27.15b the crystal is $ZnGeP_2$ (ZGP) pumped by 2.93 µm pump laser covering 4 to 12 µm range in mid-IR. In Fig.27.15.c temperature etuning of PPLN OPO output is shown -150 degrees temperature difference tune output over the range of 1.5 to 4.5µm.

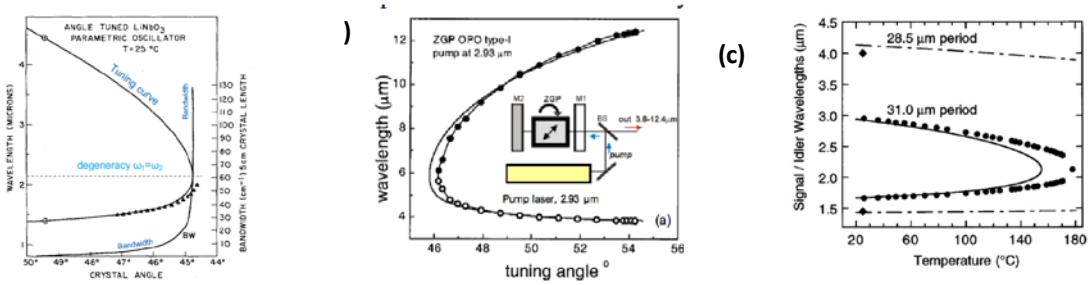

Figure 27.15. Angle tuning OPO output in (a) in $LiNbO_3$ (b) in $ZnGeP_2$ and (c)-temperature tuning of PPLN OPO

In Fig.27.16 (a) and (b) one can see how PPLN OPO can be tuned by shifting the crystal inside the resonator laterally and thus changing the nonlinear grating period.

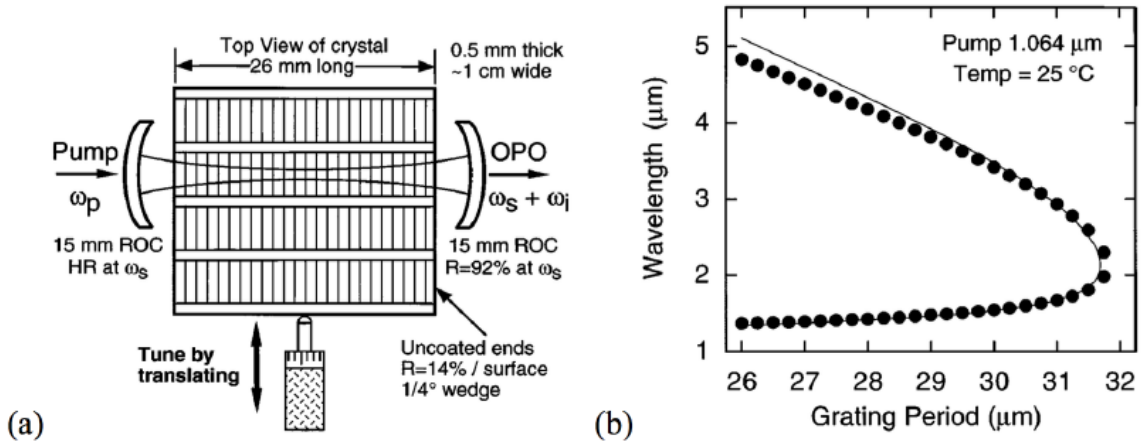

Figure 27.16 Tuning PPLN OPO by changing the grating period.